

Influence of Polymer Size on Polystyrene Biodegradation in Mealworms (*Tenebrio molitor*): Responses of Depolymerization Pattern, Gut Microbiome, and Metabolome to Polymers with Low to Ultrahigh Molecular Weight

Bo-Yu Peng, Ying Sun, Shaoze Xiao, Jiabin Chen, Xuefei Zhou, Wei-Min Wu,* and Yalei Zhang*



Cite This: *Environ. Sci. Technol.* 2022, 56, 17310–17320



Read Online

ACCESS |

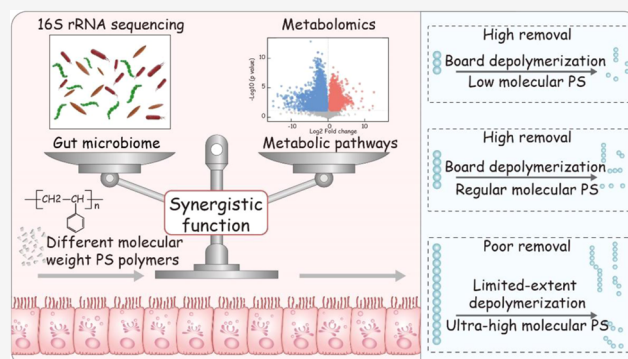
Metrics & More

Article Recommendations

Supporting Information

ABSTRACT: Biodegradation of polystyrene (PS) in mealworms (*Tenebrio molitor* larvae) has been identified with commercial PS foams. However, there is currently limited understanding of the influence of molecular weight (MW) on insect-mediated plastic biodegradation and the corresponding responses of mealworms. In this study, we provided the results of PS biodegradation, gut microbiome, and metabolome by feeding mealworms with high-purity PS microplastics with a wide variety of MW. Over 24 days, mealworms (50 individuals) fed with 0.20 g of PS showed decreasing removal of 74.1 ± 1.7 , 64.1 ± 1.6 , 64.4 ± 4.0 , 73.5 ± 0.9 , 60.6 ± 2.6 , and $39.7 \pm 4.3\%$ for PS polymers with respective weight-average molecular weights (M_w) of 6.70, 29.17, 88.63, 192.9, 612.2, and 1346 kDa. The mealworms degraded most PS polymers via broad depolymerization but ultrahigh-MW PS via limited-extent depolymerization. The gut microbiome was strongly associated with biodegradation, but that with low- and medium-MW PS was significantly distinct from that with ultrahigh-MW PS. Metabolomic analysis indicated that PS biodegradation reprogrammed the metabolome and caused intestinal dysbiosis depending on MW. Our findings demonstrate that mealworms alter their gut microbiome and intestinal metabolic pathways in response to *in vivo* biodegradation of PS polymers of various MWs.

KEYWORDS: polystyrene, molecular weight, biodegradation, mealworms, gut microbiome, metabolome



Downloaded via WASHINGTON UNIV on July 25, 2024 at 20:24:37 (UTC).
See https://pubs.acs.org/sharingguidelines for options on how to legitimately share published articles.

INTRODUCTION

The accumulation of plastic waste in the environment is a well-known risk to human and environmental health. High demand for six major polymers, *i.e.*, polystyrene (PS, 6.1%), poly(ethylene terephthalate) (PET, 8.4%), polyurethane (PUR, 7.8%), poly(vinyl chloride) (PVC, 9.6%), polypropylene (PP, 19.7%), and polyethylene (PE, 31.3%), has pushed the production of petroleum-derived polymers to near 370 million metric tons in 2020.¹ Projections indicate that plastic pollution will even treble by 2040 under a business-as-usual scenario.² PS, chemically expressed as $[-CH-(C_6H_5)CH_2-]_n$, is not structurally complex as other polymers, with no differing chain branching structure and diverse crystallinity.^{3,4} Commercial PS products are mainly atactic polymers, in which the phenyl groups are randomly distributed on both sides of the polymer chain, including expanded PS (EPS) used for building insulation, packing, *etc.*; extruded PS (XPS) used for food containers, coffee cups, *etc.*; and high-impact polystyrene (HIPS) for liquid containers, toys, *etc.* The random positioning of the atactic PS prevents the chains from aligning with enough regularity to achieve any crystallinity, making PS different from

other major polymers. Syndiotactic polystyrene (SPS), which is produced by adding different additives and varying the degree of polymerization for different commercial applications, is applied at a limited level. Plastic additives are added to PS products for various applications, but they impact plastic biodegradability.^{5–7} PS is also one of the major sources of plastic waste entering the environment, including plastic solid waste, microplastics (MPs), and nanoplastics (NPs).^{4,8–10}

Research on plastic biodegradation *via* microbial and enzymatic approaches has been performed since the 1970s.^{11–13} Microbial biodegradation of plastics in the environment is considered extremely slow, taking months or even years.⁸ The physicochemical properties of polymers impact biodegradation, with the major influencing factors

Received: August 29, 2022

Revised: October 27, 2022

Accepted: October 31, 2022

Published: November 9, 2022



Table 1. Characterization of MW Changes of the Ingested PS MPs after Passing through the Larval Intestinal Tract (Mean \pm Standard Deviation, $n = 3$)^a

	M_w (kDa)	change in M_w (%)	M_n (kDa)	change in M_n (%)	M_z (kDa)	change in M_z (%)	PDI
PS-1	6.70		6.47		6.93		1.036
PS-1 frass	6.01 \pm 0.17	-10.30 \pm 2.54	4.23 \pm 0.13	-34.62 \pm 2.01	6.59 \pm 0.11	-4.91 \pm 1.59	1.421
PS-2	29.17		27.81		30.41		1.049
PS-2 frass	26.57 \pm 0.74	-8.91 \pm 2.54	24.43 \pm 0.38	-12.15 \pm 1.37	28.54 \pm 0.13	-6.15 \pm 0.43	1.088
PS-3	88.63		84.32		94.06		1.051
PS-3 frass	80.49 \pm 1.34	-9.18 \pm 1.51	68.13 \pm 1.57	-19.20 \pm 1.86	90.44 \pm 0.86	-3.85 \pm 0.91	1.181
PS-4	192.9		182.4		210.5		1.058
PS-4 frass	155.6 \pm 4.32	-19.34 \pm 2.23	124.6 \pm 4.35	-31.69 \pm 2.38	197.4 \pm 1.10	-6.22 \pm 0.52	1.248
PS-5	612.2		561.4		678.0		1.090
PS-5 frass	566.3 \pm 11.6	-7.50 \pm 1.89	427.1 \pm 5.06	-23.92 \pm 0.90	664.8 \pm 9.72	-1.95 \pm 1.43	1.223
PS-6	1346		1268		1590		1.062
PS-6 frass	1870 \pm 48.6	+38.93 \pm 3.61	1637 \pm 30.1	+29.10 \pm 2.37	2004 \pm 21.3	+26.04 \pm 1.34	1.142

^a M_w = weight-average molecular weight; M_n = number-average molecular weight; M_z = size-average molecular weight; PDI = polydispersity index.

including the polymer type, surface hydrophobicity, molecular weight (MW), molecular-weight distribution (MWD), and physical structure.^{11,12,14–16} The polymer MW is expressed as the number-average (M_n), weight-average (M_w), and size-average molecular weight (M_z). M_n provides information about the lowest-MW fraction; M_w is the average closest to the center of the distribution curve; and M_z represents the highest-MW portion. MW and MWD remarkably affect the mechanical properties of polymers.¹⁷ In general, non-hydrolyzable plastics (PE, PP, PS, PVC, etc.) are more resistant to biodegradation than hydrolyzable polymers (PET, PUR, etc.); degradation of polymers with higher MW or higher crystallinity is likely more difficult than that of polymers with lower MW or lower crystallinity.^{12,16} Since the atactic structure of PS prevents the chains from aligning with enough regularity to achieve any crystallinity, MW has a dominant impact on PS biodegradation.

Some invertebrates voluntarily masticate various polymers, convert macroscale fragments into micron-scale particles, and display quick plastic biodegradation under *in vivo* settings. In particular, insect larvae belonging to darkling beetles (Coleoptera: Tenebrionidae) have been demonstrated to biodegrade various plastics, including the larvae of *Tenebrio molitor*, *Tenebrio obscurus*, *Zophobas atratus*, *Tribolium castaneum*, and *Plesiophthalmus davidi*.^{6,7,17–35} Among them, the most widely studied species is yellow mealworms (*T. molitor* Linnaeus 1758), which are capable of degrading major plastics including PE, PS, PP, PVC, PUR, and poly(lactic acid) (PLA),^{6,7,17,18,20–22,24–27,29,31,32,36,37} and are ideal model insect larvae for investigating plastic biodegradation since they aggressively chew and ingest plastic products (foam, film, etc.) and are also available commercially at pet markets as animal feed on a large scale due to easy rearing.^{18,31,38,39} Mealworms are holometabolic insects and go through four life stages: egg, larva, pupa, and adult beetle. Up-to-date research indicated that they biodegrade PS, PP, PVC, and PLA via a gut microbe-dependent mechanism, and low-density PE (LDPE) and high-density PE (HDPE) via a gut microbe-independent mechanism, as verified based on antibiotic suppression tests.^{7,21,22,25,27,29,32,40}

PS biodegradation by mealworms was identified in 2015, in which commercial EPS foam was used as the feedstock.¹⁸ Since then, a variety of research has been done using various PS materials, mainly EPS and XPS foams.^{6,7,18,20,22} Researchers found that mealworms secreted emulsifying factor(s) (30–100

kDa) that mediated PS bioavailability, while their gut microbiome secreted substances (<30 kDa) that increased respiration on PS, suggesting a complex synergistic metabolic process in the mealworm intestines during biodegradation.²⁴ However, the preceding research only used commercial PS products with M_w ranging from 130 to 334 kDa,^{6,7,18,20,22} which are mixed amorphous polymers with wide MWD and usually contain plastic additives such as antioxidants, antiblock compounds, and slip agents.^{5,11,12,26} Therefore, the results of these studies are comprehensive outputs of mixed polymers with broad MWD plus additives and did not provide direct insights into the biodegradation of pure PS polymers with defined MW or with narrow MWD, and plastic additives could also influence biodegradation reactions. To date, there is currently limited understanding of how MW and MWD affect PS biodegradation and the associated gut microbiome in PS-degrading mealworms, and no research has been reported on PS biodegradation using high-purity PS polymers with different defined MW, especially low vs high and ultrahigh MW. The gut microbial structure unique to the biodegradation of PS polymers with different defined MWs and the respective intestinal metabolic responses of mealworms remain unknown.

We hypothesized that biodegradation of PS with different MWs would result in distinct PS removal performance and depolymerization pattern as well as different physiological responses, gut microbiome, and intestinal metabolic pathways in mealworms, i.e., the size of polymer chains would regulate the biodegradation and endogenous metabolic activities. To test this hypothesis, we investigated PS biodegradation using six high-purity PS MPs with a wide variety of MW from low (6.70 and 29.17 kDa), medium (88.63 and 192.9 kDa), high (612.2 kDa), to ultrahigh M_w (1346 kDa); characterized the responses of the intestinal microbiome to respective PS polymers; and performed metabolomic analysis to explore the associated metabolic pathways in mealworms.

MATERIALS AND METHODS

Source of Mealworms and Materials. Mealworms and wheat bran (a normal diet to feed mealworms) were purchased from Binzhou Mealworm (Shandong, China). The main nutrients of wheat bran include proteins, dietary fiber, vitamins, and minerals.⁵¹ It also contains cellulose, hemicellulose, and lignin. The larvae were five to six instars with an average weight of 91.8 \pm 2.0 mg and an initial length of 2.1 \pm 0.2 cm (Table S1 and Figure S1). The elemental ratios (% w/w)

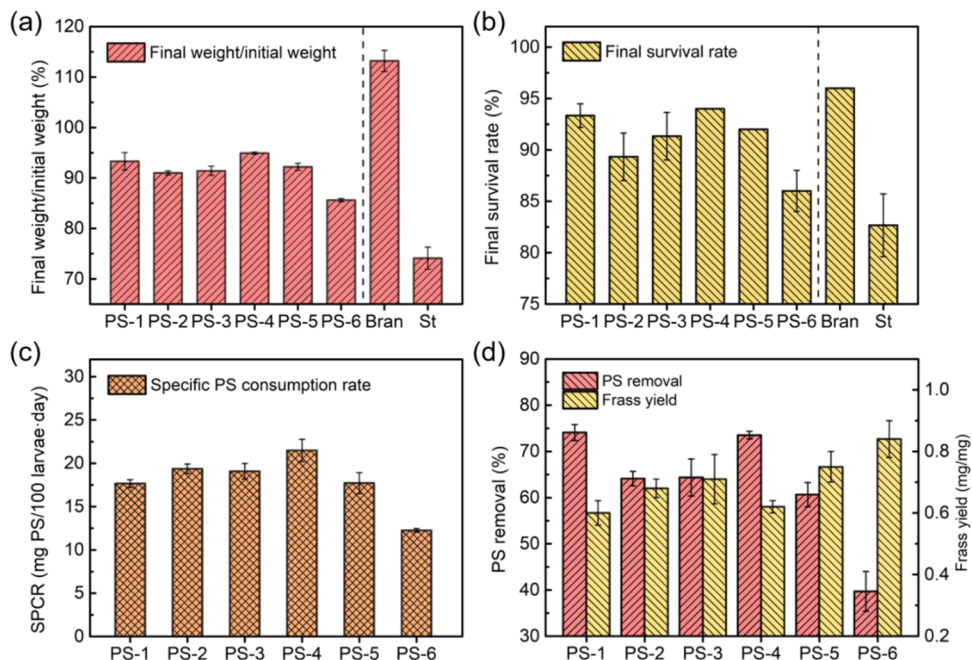


Figure 1. Physiological response of mealworms to PS MPs with different defined MW and PS removal. (a) Final weight *vs* initial weight (%) of the mealworms under different feeding conditions (day 24); initial average weight of mealworms: 91.8 ± 2.0 mg. (b) Final survival rates (%) (day 24). (c) Specific PS consumption rates (SPCRs) under different feeding conditions; the SPCR were calculated after the PS MPs in respective containers were all consumed. Within the test period (24 days), five experimental groups (PS-1, PS-2, PS-3, PS-4, and PS-5) finished the consumption of all feed, while the PS-6 group finished the consumption on day 33. (d) PS removal (%) and frass yield (ratio of frass *vs* PS MPs consumed, mg mg⁻¹) under different dietary conditions. The data were collected after the respective feeding groups finished the consumption of feedstock. St = starvation.

w) of the bran were: C, 35.71; H, 6.53; O, 41.50; N, 2.73; and S, 0.49 (Table S2). The six PS MPs were purchased from Agilent Technologies Inc., which are used as PS standards (particle diameter $<80\text{ }\mu\text{m}$) and labeled as PS-1, PS-2, PS-3, PS-4, PS-5, and PS-6 with respective M_w of 6.70, 29.17, 88.63, 192.9, 612.2, and 1346 kDa, and M_n of 6.47, 27.81, 84.32, 182.4, 561.4, and 1268 kDa (Table 1). Among these samples, PS-1 and PS-2 were low-MW PS; PS-3 and PS-4 belonged to medium-MW PS, which fit the mean MW value of most commercial PS foams; PS-5 was high-MW PS; and PS-6 was ultrahigh-MW PS. The polydispersity index ($\text{PDI} = M_w/M_n$) of all PS MPs was less than 1.09 (Table 1), indicating an extremely narrow MWD. Detailed properties of these PS MPs (Tables S3 and S4) indicated that the contents of 11 common plasticizers were below detection limits in all samples and they were free-additives. All other chemicals were purchased from Sigma-Aldrich (SI M1).

Experimental Design of PS Consumption and Biodegradation. Eight experimental groups with triplicates were tested to evaluate the consumption and biodegradation of PS in mealworms under eight feeding conditions, *i.e.*, PS-1, PS-2, PS-3, PS-4, PS-5, PS-6, bran, and starvation (St). The experimental procedures and conditions followed previously established protocols.¹⁷ Glass containers ($11.2\text{ cm} \times 11.2\text{ cm} \times 5.5\text{ cm}$) contained 50 mealworms initially, with a population density of $0.4\text{ mealworms cm}^{-2}$. All containers were kept in a laboratory thermostatic incubator at a temperature of $25 \pm 0.5^\circ\text{C}$ and a humidity of $70 \pm 5\%$.

Respective PS MPs (0.20 g) were added to each PS-fed container. The mealworms in the bran-fed containers were fed with 0.20 g of bran initially and then supplemented with 0.20 g every 8 days. At the end of the 24-day test, the final weight and

survival rate (SR) were measured. The specific PS consumption rate (SPCR) and frass yield (ratio of frass *vs* PS MPs consumed) were determined after all PS MPs were completely consumed. In this study, we chose 24 days as the test duration because petroleum-based plastics (PS, PE, PP, etc.) can provide carbon and energy sources to support the healthy life activities of the larvae for about 3–5 weeks.^{6,17–19,22,25} To obtain sufficient frass for analysis, more containers were prepared under the same conditions (SI M2). The calculation procedure was documented in SI M3.

PS Removal and Depolymerization Pattern. The PS-fed frass was collected to determine the water-extracted fraction (C_w), ethanol-extracted fraction (C_e), and THF-extracted fraction (C_t) which were used to estimate the residual PS content.¹⁷ The PS removal was calculated based on the total mass of PS consumed, the mass of frass generated, and the residual PS content in the frass (SI M4).

To characterize the change in MW and PS depolymerization pattern, gel permeation chromatography (GPC) analysis was performed to determine M_n , M_w , M_z , PDI, and MWD of the residual PS *vs* original PS MPs. The GPC analysis was performed at an ambient temperature with THF as the solvent (eluent flow rate: 0.8 mL min^{-1}). Detailed methods were documented in SI M5.

Microbial Community and Metabolomic Analysis. To investigate the gut microbiome and metabolome, the mealworms were raised as described for the biodegradation tests. After 3 weeks, the mealworms fed with PS-1 (M_w of 6.70 kDa; called PS-L), PS-4 (M_w of 192.9 kDa; called PS-M), PS-6 (M_w of 1346 kDa; called PS-H), bran, and unfed (St) were randomly selected and euthanized to retrieve the gut tissues. The three PS MPs represented PS polymers with low, medium,

and ultrahigh MW, respectively. The guts of 30 mealworms were combined and utilized as one sample. The analyses of alpha diversity, beta diversity, and microbial community structure were performed on an online cloud platform with the R package “vegan” used to assess the microbial diversity. Principal coordinate analysis (PCoA) was quantified using the Bray–Curtis dissimilarity. The methods for gut microbial analysis were documented in SI M6.^{31,34}

To assess the changes in metabolic pathways in the intestines, the gut tissues from mealworms fed with PS-L, PS-M, PS-H, and bran were utilized to conduct metabolomics analysis using the gas chromatograph coupled with a time-of-flight mass spectrometer (GC-TOF-MS) and liquid chromatography–tandem mass spectrometry (LC-MS/MS) (SI M7).^{41,42} Human metabolome database (HMDB) and Kyoto Encyclopedia of Genes and Genomes (KEGG) databases were used for metabolite annotation. The metabolites with an adjusted *p*-value < 0.05 and VIP > 1 were considered significantly different.

Statistical Analysis. Statistical analysis of variance (ANOVA) was used to compare the physiological responses of mealworms, SPCRs, and PS removal using Origin Pro 2021 (Origin Lab Corp.). The variations in the M_n , M_w , M_z , and PDI were analyzed by pairwise comparisons using the Student's *t* test with Tukey's correction. The results were expressed as mean ± standard deviation.

RESULTS AND DISCUSSION

PS Consumption and Physiological Responses of Mealworms. Changes in the average weight and the SRs of mealworms after 24 days are shown in Figure 1a. No weight growth was observed in the mealworms fed with PS MPs as the sole diet, as observed previously.^{6,7,25} Weight loss of mealworms appeared to be increased as PS MW increased, *i.e.*, the ratio of final weight/initial weight was 93.3 ± 1.7 , 91.0 ± 0.3 , 91.4 ± 0.9 , 94.9 ± 0.2 , 92.2 ± 0.7 , and $85.6 \pm 0.3\%$ for the larvae fed with PS-1, PS-2, PS-3, PS-4, PS-5, and PS-6, respectively. For comparison, the ratio of the starvation control group was $74.1 \pm 2.2\%$, while that of the bran-fed mealworms increased by $13.0 \pm 2.1\%$ due to growth on their normal feed (Figure 1a). The results suggested that mealworms fed with PS MPs with low to high, even ultrahigh-MW PS (*i.e.*, M_w of 6.70–612.2, and 1346 kDa or PS-1 to PS-6) obtained energy sources to maintain their life activities and consumed fewer body storage materials (fats, proteins, *etc.*), while starved mealworms consumed their body biomass for survival. Similar observations were found in mealworms fed with commercial EPS and XPS foams with MWs ranging from 130 to 334 kDa as the sole diet due to the fact that they digested PS as an energy and carbon source effectively.^{7,18,22} The observation of increasing weight loss as the MW increased (Figure 1a), particularly for the mealworms fed with ultrahigh-MW PS MPs (PS-6), was likely due to decreasing digestibility of the PS MPs and thus less energy source received from the higher-MW PS. In the gut luminal environment, feeding a plastic diet alone would cause nutrient deficiency and a lack of mineral elements necessary for enzyme synthesis, resulting in reduced nutrient acquisition capability.⁴³ This would, in turn, compromise the mealworm growth as observed in this study (Figure 1a). The influence of supplementation of co-diet bran on the survival of mealworms with PS polymers with different MWs should be detailed in future studies.

On day 24, the SRs of the respective groups were: PS-1, 93.3 ± 1.2%; PS-2, 89.3 ± 2.3%; PS-3, 91.3 ± 2.3%; PS-4, 94.0 ± 0.0%; PS-5, 92.0 ± 0.0%; PS-6, 86.0 ± 2.0%; bran-fed, 96.0 ± 0.0%; and starvation, 82.7 ± 3.1% (Figure 1b). The mealworms fed with PS-1, PS-2, PS-3, PS-4, and PS-5 had similar high SRs (>~90%), but their SRs were significantly higher (*p* < 0.05) than those of the PS-6 and starvation groups and slightly lower than that of the bran-fed as expected. In this study, cannibalism was observed in the PS-fed and starved mealworms but not in the bran-fed group. Therefore, the lower SRs of the PS-fed and starved mealworms could be partially attributed to innate cannibalistic behavior and malnutrition over time, especially under starvation conditions.

SPCRs were determined after mealworms completely consumed all PS MPs on the basis of the mass of PS MPs ingested per 100 larvae per day.^{17,25,29} The mealworms in the PS-1 to PS-5 groups completely consumed all of the PS MPs prior to day 24, but the PS-6 group finished the consumption until day 33. After the consumption of all of the PS MPs, the mealworms tried to hide inside the frass layer and ingested the frass as food. The SPCR was relatively high for the mealworms fed with PS-1 to PS-5 MPs (Figure 1c), and a peak rate of 21.5 ± 1.3 mg PS 100 larvae⁻¹ d⁻¹ (or 2.34 ± 0.14 mg PS g larvae⁻¹ d⁻¹) was found in the PS-4 group (M_w of 192.9 kDa). The lowest rate of 12.2 ± 0.2 mg PS 100 larvae⁻¹ d⁻¹ (or 1.33 ± 0.02 mg PS g larvae⁻¹ d⁻¹) was performed by the PS-6 group (M_w of 1346 kDa). The respective SPCR of PS-1, PS-2, PS-3, and PS-5 groups was 17.7 ± 0.5 , 19.4 ± 0.5 , 19.1 ± 0.9 , and 17.7 ± 1.2 mg PS 100 larvae⁻¹ d⁻¹ (Table S5). The results suggested clearly that mealworms exhibited higher affinity for the diets of PS MPs with low (PS-1 and PS-2), medium (PS-3 and PS-4), and high (PS-5) MWs than that with ultrahigh MW (PS-6). However, the reason for the difference in SPCRs among PS-1 to PS-5 was not clear and might be due to other unknown physical factors. In this study, we did find that the ultrahigh MW of PS appeared to influence SPCR negatively, and the low-MW PS to high-MW PS, which basically fits the range of commercial PS foams with broad MWD, was favorable. All SPCRs in this study are basically in line with previous biodegradation studies using commercial PS foams (M_w from 130 to 334 kDa) by mealworms from various sources around the world at $8.5\text{--}20.7$ mg PS 100 larvae⁻¹ d⁻¹.^{6,7,22,29} The SPCRs could be influenced by many factors, including the incubation conditions, properties of the tested PS materials, source of mealworms, mealworm instars and larval size, test temperature, humidity, *etc.*

Mass Balance and PS Removal. The mass balance and PS removal were estimated on the basis of the mass of ingested PS, the mass of egested frass, and water-, ethanol-, and THF-extracted fractions (C_w , C_e , and C_t). The frass yield, an indirect indicator of digestibility, was 0.60, 0.68, 0.71, 0.62, 0.75, and 0.84 for the mealworms fed with PS-1 to PS-6 MPs, respectively. In general, the PS MPs with the lower MW resulted in the relatively lower frass yield (Figure 1d), suggesting that the lower the MW, the more PS polymers were digested or degraded.

The C_w value indicated the fraction of hydrophilic, digested organic components, and salts in the frass; the C_e value indicated the fraction of lipophilic substances in the frass; and the C_t value indicated the residual and modified PS content in the frass. Therefore, the C_t value was used to estimate residual PS polymers in the frass.¹⁷ All frass samples from the mealworms fed with PS diets had a high level of the water-

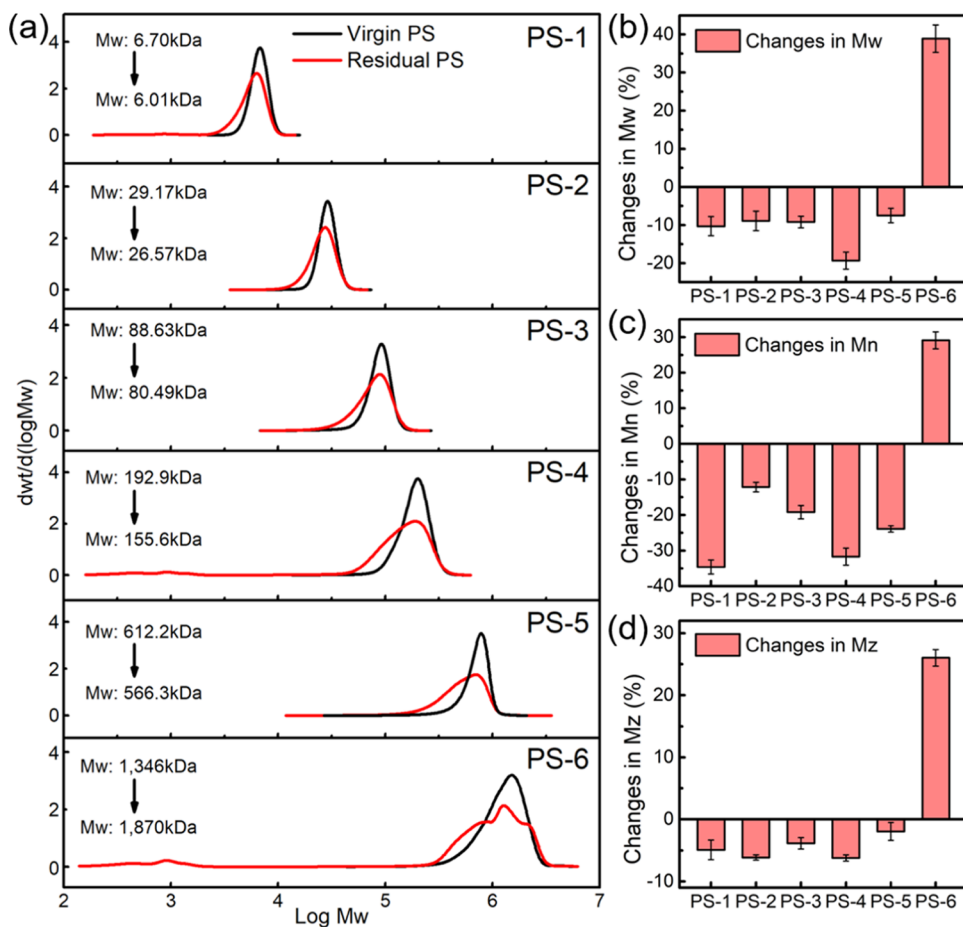


Figure 2. Changes in molecular weight (MW) and molecular-weight distribution (MWD) of the ingested PS polymers in the mealworms. (a) Shift of the MWD of the ingested PS with different MWs. Black lines indicate the MWD of original PS polymers, while red lines represent the MWD of the residual PS polymers extracted from frass samples. Changes in (b) M_w , (c) M_n , and (d) M_z values after the ingested PS MPs went through the larval gut. M_w = weight-average molecular weight; M_n = number-average molecular weight; M_z = size-average molecular weight.

extracted fraction ($C_w > 15\%$) (Table S6 and Figure S2). The C_w values of the PS-1 to PS-6 groups were as high as 25.5 ± 0.5 , 25.5 ± 0.5 , 19.3 ± 1.7 , 20.1 ± 0.4 , 23.7 ± 1.6 , 19.8 ± 0.3 , and $18.9 \pm 0.3\%$, respectively. The results suggested that the mealworms converted significant amounts of PS polymers to water-soluble intermediates. The ethanol-extracted fraction, on the other hand, varied between $1.5 \pm 0.1\%$ (PS-6 group) and $3.3 \pm 0.2\%$ (PS-1 group). The highest C_e value was obtained in the PS-1 group (M_w of 6.70 kDa), which might be related to that the digestion of low-MW PS (e.g., $M_w < 10$ kDa) generated slightly more lipophilic compounds.

The C_t value was an indirect parameter to represent the residual PS in frass. For the PS-1 to PS-6 groups, the C_t values were 43.2 ± 1.2 , 52.8 ± 3.9 , 50.2 ± 2.4 , 42.7 ± 1.8 , 52.5 ± 0.9 , and $71.8 \pm 3.7\%$, respectively (Figure S2), and the respective PS removal was estimated as at 74.1 ± 1.7 , 64.1 ± 1.6 , 64.4 ± 4.0 , 73.5 ± 0.9 , 60.6 ± 2.6 , and $39.7 \pm 4.3\%$ (Figure 1d and Table S6). Interestingly, the PS removal efficiency was both high (>70%) for the PS-1 (M_w of 6.70 kDa) and PS-4 (M_w of 192.9 kDa) MPs. Commercial PS foams with M_w ranging from 130 to 334 kDa were efficiently removed by mealworms from various sources from China, the United States, and the United Kingdom,^{6,7,18,22,25,29} implying that mealworms have a prominent capability to effectively digest PS polymers with medium MW in their digestive intestines. In this study, the highest PS removal ($74.1 \pm 1.7\%$) was observed for low-MW

PS MPs (PS-1) and relatively high removal ($60.6 \pm 2.6\%$) was still obtained with high-MW PS (PS-5). However, the mealworms fed with ultrahigh-MW PS MPs (PS-6) had relatively poor PS removal of $39.7 \pm 4.3\%$ (Figure 1d). The results suggested that PS polymers from low to high MW can be effectively biodegraded, but ultrahigh-MW polymers (>1000 kDa) would be challenging to digest and depolymerize, which is consistent with the studies on the enzymatic degradation of PET, *i.e.*, MW impacts plastic degradation.^{11,12}

Effects of Molecular Weight on PS Depolymerization Patterns.

In this study, we used only GPC analysis to demonstrate PS depolymerization and biodegradation because previous studies confirmed that commercial PS can be oxidized and biodegraded by mealworms *via* other analyses, including Fourier transform infrared spectroscopy (FTIR), proton nuclear magnetic resonance (^1H NMR), thermogravimetric analysis (TGA), etc.^{6,7,18} The MWD and depolymerization patterns were characterized by comparing the residual PS in frass with virgin PS MPs. The MWD of all PS MPs was shifted after biodegradation (Figure 2a) with significant changes in M_w , M_n , and M_z observed (Figure 2b–d).

The MWD of all PS polymers with low to ultrahigh MWs shifted toward a low-MW direction after the PS passed through the intestines of mealworms. The generation/accumulation of lower-MW-chain polymers after biodegradation was clearly observed even in ultrahigh-MW PS-6 (Figure 2a). This

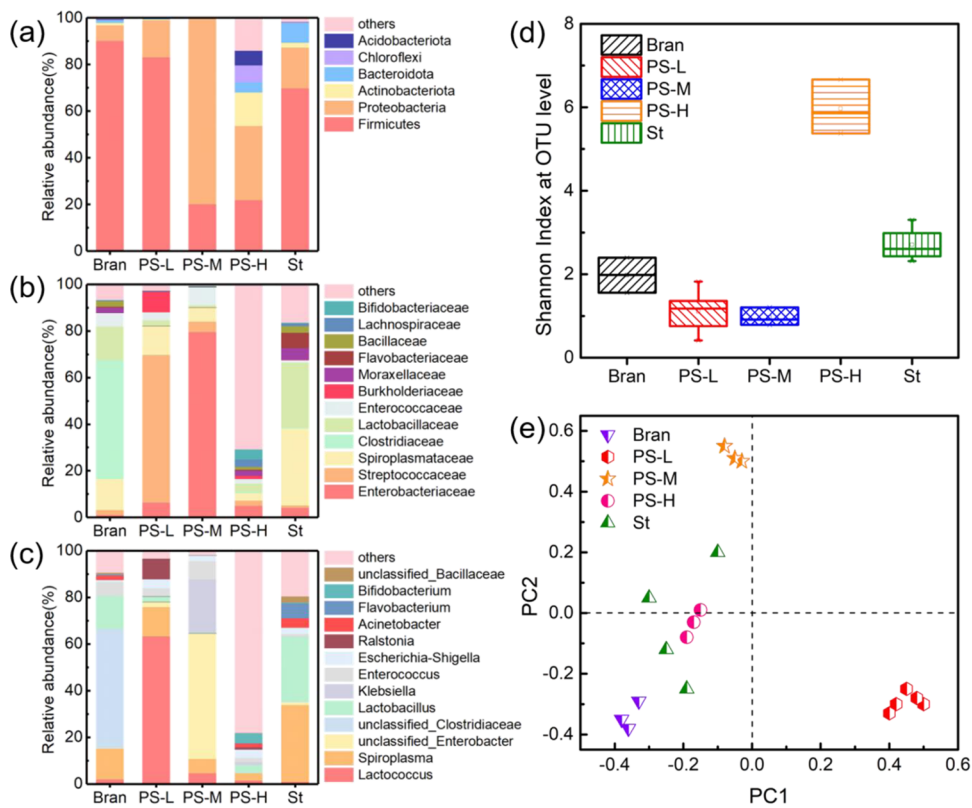


Figure 3. Analysis of the gut microbiome of mealworms under different feeding conditions (Bran, PS-L, PS-M, PS-H, St). Relative abundance at the (a) phylum level, (b) family level, and (c) genus level. Relative abundance was shown in the mean value. “Others” are the gut microbes with relative abundance lower than 0.01. (d) Shannon index of the gut microbiome under different feeding conditions. (e) Principal coordinate analysis (PCoA) based on illumina sequencing of the gut microbiome of mealworms under different feeding conditions.

confirmed that all PS MPs tested were depolymerized. The M_w of residual polymers of PS-1, PS-2, PS-3, PS-4, and PS-5 groups significantly decreased by 10.30 ± 2.54 , 8.91 ± 2.54 , 9.18 ± 1.51 , 19.34 ± 2.23 , and $7.50 \pm 1.89\%$, respectively; M_n declined by 34.62 ± 2.01 , 12.15 ± 1.37 , 19.20 ± 1.86 , 31.69 ± 2.38 , and $23.92 \pm 0.90\%$, respectively; and M_z reduced by 4.91 ± 1.59 , 6.15 ± 0.43 , 3.85 ± 0.91 , 6.22 ± 0.52 , and $1.95 \pm 1.43\%$, respectively. These data implied that the PS polymer chains were significantly reduced. The depolymerization fit the typical broad depolymerization (BD) pattern for all PS MPs with low to high MW, which was observed during the biodegradation of commercial PS foams with M_w from 130 to 334 kDa by mealworms in China, the United States, and the United Kingdom.^{6,7,18,22,25,29} Therefore, we conclude that the BD pattern is likely ubiquitous for mealworms to degrade PS polymers with low to high MW (e.g., $M_w < \sim 600$ kDa), although the depolymerization extent was different. We also noticed that the M_z of the high-MW PS polymer (PS-5) only decreased by $1.95 \pm 1.43\%$ from 678.0 to 664.8 kDa (Table 1), indicating that the highest-MW portion was indeed challenging for degradation.

For the PS MPs with ultrahigh MW (M_w of 1,346 kDa), the shift of MWD of the residual polymers was still toward a low-MW direction (Figure 2a). However, the depolymerization pattern was different and showed limited-extent depolymerization (LD), i.e., the M_w , M_n , and M_z of the residual PS significantly increased by 38.93 ± 3.61 , 29.10 ± 2.37 , and $26.04 \pm 1.34\%$, respectively (Figure 2b–d). This was also observed in LDPE biodegradation.²⁷ The limited-extent depolymerization pattern (the increase in the M_w , M_n , and

M_z) was likely related to the selective depolymerization and degradation of lower-molecular polymers at higher rates than large molecular portions, i.e., the functional enzymes and gut bacteria in the mealworms efficiently attacked PS polymers with short chains of low and medium MW in nonspecific ways throughout the biodegradation process but reacted slowly with PS polymers with long chains of high and ultrahigh MW. Thus, more portions of high-MW PS polymers remained in the frass, resulting in an increase in M_w , M_n , and M_z , although depolymerization occurred and the broadness of MWD increased (Figure 2a). The observation of limited-extent depolymerization was reported during LDPE degradation in mealworms;²² PS degradation in superworms (*Z. atratus*),³⁰ microbial PUR biodegradation by a landfill microbial culture;⁵² PS degradation in greater waxworms (*G. mellonella*);³⁴ and digestion of PS foam by land snails *Achatina fulica*.⁵³

The PDI indicated the change of heterogeneity in chain-length distributions of tested polymers.^{12,20,27,30,31} The original PDI of the tested PS ranged from 1.036 to 1.090 (Table 1). After biodegradation, the PDI of all residual PS polymers increased: PS-1 from 1.036 to 1.421, PS-2 from 1.049 to 1.088, PS-3 from 1.051 to 1.181, PS-4 from 1.058 to 1.248, PS-5 from 1.090 to 1.223, and PS-6 from 1.062 to 1.142. The results are consistent with the observations that the MWD of all residual PS polymers shifted (Figure 2a). This suggested the occurrence of endo-type depolymerization or random internal scission of chains in polymer macromolecules, which generated oligomeric products and mid-chain polymers and finally yielded residual polymers with heterogeneous MWD.^{5,27,43}

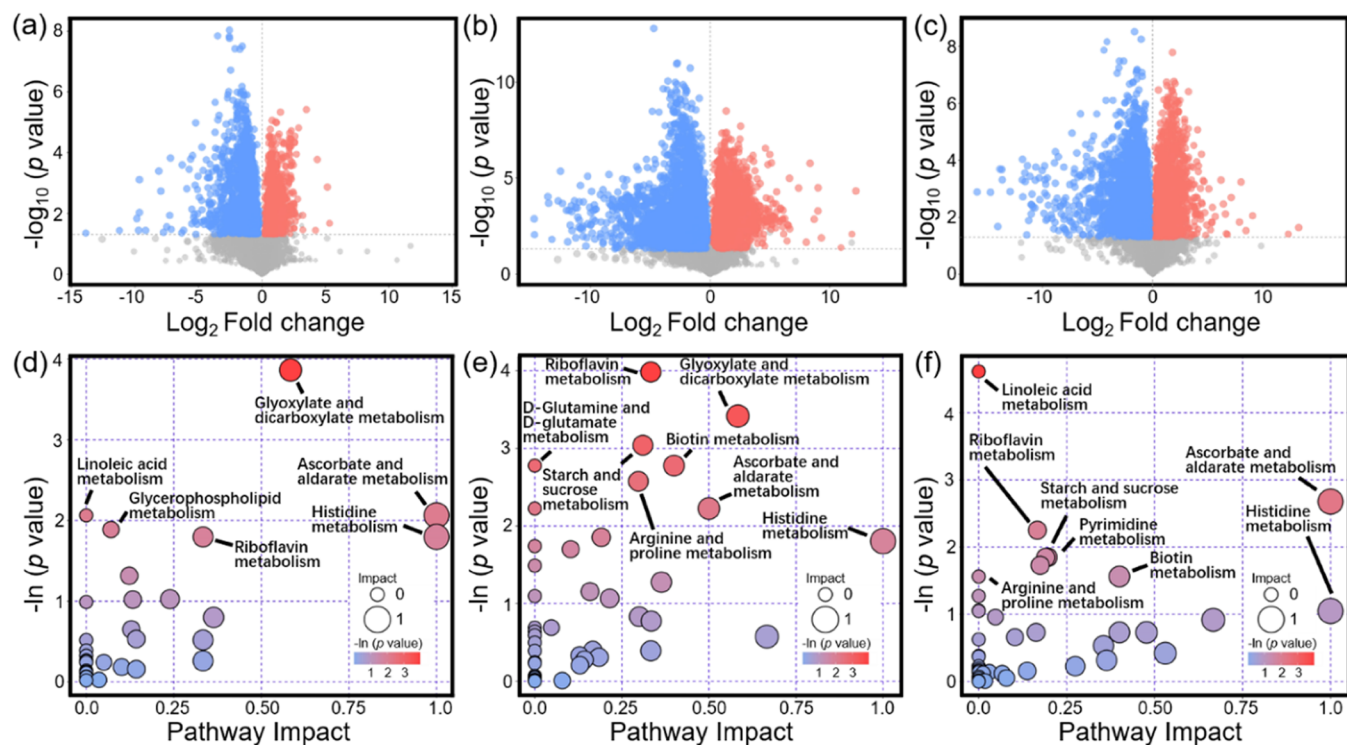


Figure 4. Comparative metabolomic analysis of the guts of mealworms under different feeding conditions. The volcano map of the metabolites in the gut of mealworms from the (a) PS-L, (b) PS-M, and (c) PS-H experimental groups; pathway analysis of the metabolic profiles in the mealworm gut from the (d) PS-L, (e) PS-M, and (f) PS-H experimental groups. Each bubble in the figures represents an enriched metabolic pathway in the mealworms. The size and the abscissa of the bubble indicate the influence intensity of the metabolic pathway according to topological analysis (TA), i.e., the larger the bubble, the greater the influence. The ordinate and the color intensity of bubbles show the significant *p* value of enriched metabolic pathways. The metabolites with an adjusted *p*-value < 0.05 and VIP > 1 were considered significantly different.

Gut Microbial Analysis. To evaluate the gut microbiome in response to *in vivo* biodegradation of PS with different MW, we performed gut microbial analysis of the mealworms fed with three selected PS MPs, *i.e.*, low MW (PS-1 with M_w of 6.70 kDa, named PS-L), medium MW (PS-4 with M_w of 192.9 kDa, named PS-M), and ultrahigh MW (PS-6 with M_w of 1346 kDa, named PS-H) *vs* mealworms fed with bran and unfed. Rarefaction curves suggested that the amplicon quality was guaranteed (Figure S3) with the sequencing information presented in Table S7.

Bacteria belonging to the phylum Firmicutes, Proteobacteria, Actinobacteria, Bacteroidetes, Chloroflexi, and Acidobacteriota dominated the gut microbiome in the mealworms (Figure 3a). Firmicutes was the most prevalent phylum in mealworms fed with bran (90.13%) and PS-L (83.15%), which was associated with the low MW of both diets. In contrast, the relative abundance of Firmicutes in the PS-M and PS-H groups was as low as 20.13 and 21.84%, respectively. Meanwhile, the phylum Proteobacteria became dominant in both PS-M and PS-H groups, increasing from 6.63 to 79.77 and 31.85%, respectively (Figure 3a). The major alteration in the gut microbiome at the family level was mostly associated with Enterobacteriaceae, Streptococcaceae, and Spiroplasmataceae after feeding PS polymers with the low and medium MW (Figure 3b). Specifically, the family Streptococcaceae was the most abundant (63.33%) in the PS-L group, while the family Enterobacteriaceae was the most abundant (79.48%) in the PS-M group. The remarkable increase in relative abundance of the family Streptococcaceae in the PS-L group was contributed by the genus *Lactococcus* (Figure 3c) which is a facultative

anaerobic fermentative microbe.^{31,44} Previous research found that the *Lactococcus* genus was strongly associated with PLA degradation, a bio-based biodegradable plastic with low MW and crystallinity.³¹ Future studies are needed to verify the role of this bacterial genus in the biodegradation of low-MW PS. On the other hand, the bacterial family Enterobacteriaceae has been reported to be associated with the depolymerization and biodegradation of various plastics (*e.g.*, PP, PVC, LDPE, and PS) in Tenebrionidae insects, especially commercial PS foams.^{7,21,22,25,29,32} Therefore, the biodegradation of PS-M could be contributed by the family Enterobacteriaceae, which participated in the breaking down and biodegradation of PS and intermediates (Figure 3b).

On the other hand, the gut microbiome of mealworms fed with ultrahigh-MW PS (PS-H) had a more complicated microbial community than those fed with PS-L and PS-M (Figure 3). Gut bacteria with low relative abundance (<1%) contributed to about 70% of the community at family level (Figure 3b), suggesting that the biodegradation of ultrahigh-MW PS polymers required complex synergistic microbial consortia. The Shannon index was used to investigate the richness and diversity of the gut microbiome. The Shannon index of the mealworms fed with PS-L and PS-M was at a similar level, which was slightly lower than that of the bran-fed and starved groups, while those fed with PS-H were remarkably higher than all other groups (Figure 3d). The results indicated that the low- and medium-MW PS resulted in gut microbiome of low taxonomic diversity and microbial complexity in the mealworms, but ultrahigh-MW PS caused high taxonomic diversity. Besides, wheat bran contains a

certain amount of carbohydrates, fat, proteins, and vitamins,^{6,7} thus resulting in a relatively complex functional gut microbiome in bran-fed mealworms.

Principal coordinate analysis (PCoA) was performed to further compare the gut microbial communities (**Figure 3e**). Four distinct clusters (bran, PS-L, PS-M, and PS-H) were separated from each other, implying that the gut microbial structure in the respective groups was significantly different. This finding also revealed that the mealworms developed their gut microbiome in response to the biodegradation of the same polymers with different MW. Interestingly, the gut microbial community of the starvation mealworms was also more diversified, *i.e.*, no cluster was developed, which could be attributable to the ingestion of frass, molted skeletons (containing chitin), dead mealworms, and digestion of body biomass (including fats, proteins, *etc.*) throughout the test period (**Figure 3e**).

Metabolic Pathway Analysis. Alterations in the metabolomic profiles and metabolic pathways of the mealworms under different diet conditions were analyzed. Compared with the bran-fed mealworms, metabolites in the intestines of mealworms fed with PS-L (**Figure 4a**), PS-M (**Figure 4b**), and PS-H (**Figure 4c**) were all differentially expressed according to the volcano map analysis. Specifically, 90, 190, and 196 differentially expressed metabolites were upregulated in the PS-L, PS-M, and PS-H groups, respectively, while 198, 306, and 221 differentially expressed metabolites were downregulated.

These differentially expressed metabolites were screened, and related pathways of the metabolic profiles were analyzed based on topological analysis (TA). The results of the pathway analysis were displayed in bubble diagrams (**Figure 4d–f**). In general, metabolic pathways were perturbed across the mealworm groups fed with low (PS-L, M_w of 6.70 kDa)-, medium (PS-M, M_w of 192.9 kDa)-, and ultrahigh (PS-H, M_w of 1,346 kDa)-MW PS polymers. Interestingly, riboflavin metabolism, histidine metabolism, and ascorbate and aldarate metabolism were significantly perturbed under all three PS feeding conditions (**Figure 4d–f**). Riboflavin could provide more electron shuttles and redox mediators that facilitated the extracellular electron transfer.^{45,46} Histidine metabolism was associated with a series of metabolic pathways, including the pentose phosphate pathway, alanine metabolism, and glutamate metabolism.⁴⁷ Therefore, comparative metabolomic analysis implied that innate metabolic mechanisms in the mealworm intestines could coordinate redox capability to complete biodegradation of PS polymers with different MWs synergistically. These findings also revealed that the mealworms might use their endogenous metabolic material reserves to compensate for the lack of nutrients, thus performing PS depolymerization and biodegradation processes.

On the other hand, distinct differential metabolic pathways were observed in the mealworms under different diet conditions. Glyoxylate and dicarboxylate metabolism was significantly perturbed in both groups fed with low (PS-L)- and medium (PS-M)-MW PS polymers (**Figure 4d,e**), but was less significant in the mealworms fed with ultrahigh (PS-H)-MW PS polymers (**Figure 4f**). Glyoxylate and dicarboxylate metabolism belong to key energy metabolism pathways,^{41,42,48} and might be strongly associated with biodegradation of PS polymers with low and medium MW and metabolism of degradation intermediates with relatively low MW. Starch and sucrose metabolism were also significantly perturbed in the mealworms fed with medium- and ultrahigh-MW PS polymers

(**Figure 4e,f**), but were less significant in the mealworms fed with low-MW PS. This could be attributed to the differences in PS polymer macrostructures and explain the distinctive depolymerization patterns in the guts of mealworms. Further research is needed to verify these perspectives by identifying and investigating the activities of putative PS degrading enzymes and the catalytic mechanisms of these enzymes for PS biodegradation processes.

Several typical metabolic pathways involved in molecular protection and oxidative stress defense (*e.g.*, in zebrafish and mice) have been found significantly altered (**Figure 4d–f**). For instance, ascorbate and aldarate metabolisms were significantly perturbed in all three mealworm groups, which contributed to maintaining the internal redox balance and defending potential oxidative stress.⁴⁹ Arginine and proline metabolism, which played a role in the maintenance of osmotic equilibrium and the interaction with enzymes to protect the structure of proteins,⁴⁶ were significantly perturbed in the mealworms fed with PS-M and PS-H. Pyrimidine metabolism, an essential metabolic pathway for RNA and DNA synthesis, membrane lipid biosynthesis, and protein glycosylation,⁵⁰ was found to be significantly perturbed only in the mealworms fed with the ultrahigh-MW PS. In addition, linoleic acid metabolism and glycerophospholipid metabolism, which were associated with membrane integrity repairment and the composition of active substances on the membrane surface, were also observed.^{41,42} Interestingly, these metabolic pathways were more prevalent in the mealworms fed with the ultrahigh-MW PS (**Figure 4f**). Previous research has indicated that microplastic ingestion could induce possible gut epithelium damage, which led to inflammation and multiple responses of the immune system in various insect species.⁴³ We hypothesized that although mealworms were capable of biodegrading PS polymers with various MWs, the uptake of PS MPs still reprogrammed the metabolic pathways within the intestinal environments, resulting in intrinsic metabolic dysbiosis in the mealworms (especially when fed with ultrahigh-MW polymers), including inducing oxidative stress, damaging antioxidant systems and membranes to some extent, as well as impacting the energy supply of mealworms and modulating their growth. Future studies will be needed to verify this hypothesis and understand the complex mechanisms concerning the impacts of MP-induced damage on the PS biodegradation process in mealworms.

Environmental Implications. This work is the first report on the biodegradation of high-purity PS with a variety of defined MWs from low to ultrahigh MW (6.70–1346 kDa) in mealworms (*T. molitor* larvae) and has confirmed that PS polymers up to 1300 kDa can be depolymerized and biodegraded. The results indicated that the gut microbiome and intestinal metabolic pathways were altered instinctively in response to *in vivo* biodegradation of PS polymers *via* different polymerization patterns. Mealworms exhibited distinct affinity, consumption rates, and removal efficiencies depending on the polymer MWs. PS MPs with M_w below 612.2 kDa were degraded *via* broad depolymerization, while PS MPs with ultrahigh MW were degraded *via* limited-extent depolymerization. These results indicate that biodegradation of commercial PS products with MW lower than 600 kDa can be performed efficiently, but biodegradation of PS with ultrahigh MWs (*e.g.*, >1000 kDa) is still challenging. According to our previous study, commercial EPS foam contained less than 1% of polymers with MW > 1000 kDa.³⁰ Our results suggest that

polymer manufacturing should further reduce or eliminate the high- to ultrahigh-MW fraction in commercial PS products in order to improve biodegradability of PS products.

The biodegradation of PS polymers with low, medium, and ultrahigh MWs resulted in different functional gut microbiomes associated with plastic biodegradation. Mealworms fed with low- and medium-MW PS had similar gut microbiomes with relatively low diversity, whereas those fed with ultrahigh-MW PS had significantly different microbiomes with high taxonomic diversity. Endogenous metabolic reserves and profiles in mealworms were also reprogrammed to coordinate redox capabilities to complete PS biodegradation processes synergistically. These findings provide new insights into understanding insect-mediated plastic biodegradation as well as the methodological capabilities to evaluate this process in both natural and engineering settings.

■ ASSOCIATED CONTENT

Supporting Information

The Supporting Information is available free of charge at <https://pubs.acs.org/doi/10.1021/acs.est.2c06260>.

Morphology of tested mealworms (Figure S1); extracted fractions in the frass egested from mealworms under PS dietary conditions (Figure S2); rarefaction curves of the Shannon index of gut bacteria (Figure S3); detailed physiological features of the mealworms (Table S1); elemental ratios of the natural wheat bran (Table S2); detailed properties of the tested standard PS powders (Table S3); plasticizer content in tested PS powders (Table S4); SPCRs under different feeding conditions (Table S5); C_w , C_e , and C_t values of the frass samples, frass yield, and PS removal by the mealworms (Table S6); and overview of basic information about the samples in gut microbial analysis (Table S7) ([PDF](#))

■ AUTHOR INFORMATION

Corresponding Authors

Wei-Min Wu — Department of Civil and Environmental Engineering, William & Cloy Codiga Resource Recovery Center, Center for Sustainable Development & Global Competitiveness, Stanford University, Stanford, California 94305-4020, United States; Phone: +1517-775-6428; Email: Billwu@stanford.edu

Yalei Zhang — State Key Laboratory of Pollution Control and Resource Reuse, College of Environmental Science and Engineering, Tongji University, Shanghai 200092, China; [orcid.org/0000-0002-3254-8965](#); Phone: +86 21 65985811; Email: Zhangyalei@tongji.edu.cn

Authors

Bo-Yu Peng — State Key Laboratory of Pollution Control and Resource Reuse, College of Environmental Science and Engineering, Tongji University, Shanghai 200092, China

Ying Sun — State Key Laboratory of Pollution Control and Resource Reuse, College of Environmental Science and Engineering, Tongji University, Shanghai 200092, China

Shaoze Xiao — State Key Laboratory of Pollution Control and Resource Reuse, College of Environmental Science and Engineering, Tongji University, Shanghai 200092, China

Jiabin Chen — State Key Laboratory of Pollution Control and Resource Reuse, College of Environmental Science and

Engineering, Tongji University, Shanghai 200092, China;

[orcid.org/0000-0002-4790-5873](#)

Xuefei Zhou — State Key Laboratory of Pollution Control and Resource Reuse, College of Environmental Science and Engineering, Tongji University, Shanghai 200092, China; [orcid.org/0000-0001-6521-0592](#)

Complete contact information is available at: <https://pubs.acs.org/10.1021/acs.est.2c06260>

Notes

The authors declare no competing financial interest.

■ ACKNOWLEDGMENTS

The authors gratefully acknowledge support from the Shanghai Gaofeng & Gaoyuan Project for University Academic Program Development (no. 22-6), the Science and Technology Commission of Shanghai Municipality (STCSM, no. 20dz1203600), the National Natural Science Foundation of China (NSFC, U21A20322), and the Woods Institute for Environment at Stanford University (Award 1197667-10-WTAZB). They thank Professor Craig S. Criddle, Stanford University, for the suggestions during this study. They also thank Ziyan Huang from Shiyanjia Lab (www.shiyanjia.com) for the biological analysis.

■ NOMENCLATURE

BD	broad depolymerization
C_e	ethanol-extracted fraction
C_t	THF-extracted fraction
C_w	water-extracted fraction
EPS	expanded polystyrene
FTIR	fourier transform infrared spectroscopy
GPC	gel permeation chromatography
^1H NMR	proton nuclear magnetic resonance
LD	limited-extent depolymerization
LDPE	low-density polyethylene
MPs	microplastics
M_n	number-average molecular weight
MW	molecular weight
M_w	weight-average molecular weight
M_z	size-average molecular weight
MWD	molecular weight distribution
NPs	nanoplastics
PCoA	principal coordinate analysis
PDI	polydispersity index
PE	polyethylene
PET	polyethylene terephthalate
PLA	polylactic acid
PP	polypropylene
PS	polystyrene
PUR	polyurethane
PVC	polyvinyl chloride
SPCR	specific PS consumption rate
SR	survival rate
THF	tetrahydrofuran
TGA	thermogravimetric analysis
XPS	extruded polystyrene

■ REFERENCES

- (1) Plastics Europe. Plastics-The facts, 2021. <https://plasticseurope.org/knowledge-hub/plastics-the-facts-2021/> (accessed Oct 21, 2022).

- (2) Allen, D.; Allen, S.; Abbasi, S.; Baker, A.; Bergmann, M.; Brahney, J.; Butler, T.; Duce, R. A.; Eckhardt, S.; Evangelou, N.; Jickells, T.; Kanakidou, M.; Kershaw, P.; Laj, P.; Levermore, J.; Li, D.; Liss, P.; Liu, K.; Mahowald, N.; Masque, P.; Materić, D.; Mayes, A. G.; McGinnity, P.; Osvath, I.; Prather, K. A.; Prospero, J. M.; Revell, L. E.; Sander, S. G.; Shim, W. J.; Slade, J.; Stein, A.; Tarasova, O.; Wright, S. Microplastics and nanoplastics in the marine-atmosphere environment. *Nat. Rev. Earth Environ.* **2022**, *3*, 393–405.
- (3) Wilkes, R. A.; Aristilde, L. Degradation and metabolism of synthetic plastics and associated products by *Pseudomonas* sp.: capabilities and challenges. *J. Appl. Microbiol.* **2017**, *123*, 582–593.
- (4) Geyer, R.; Jambeck, J. R.; Law, K. L. Production, use, and fate of all plastics ever made. *Sci. Adv.* **2017**, *3*, No. e1700782.
- (5) Taghavi, N.; Udagama, I. A.; Zhuang, W. Q.; Baroutian, S. Challenges in biodegradation of non-degradable thermoplastic waste: from environmental impact to operational readiness. *Biotechnol. Adv.* **2021**, *49*, No. 107731.
- (6) Yang, S.-S.; Wu, W.-M.; Brandon, A. M.; Fan, H. Q.; Receveur, J. P.; Li, Y.; Wang, Z. Y.; Fan, R.; McClellan, R. L.; Gao, S. H.; Ning, D.; Phillips, D. H.; Peng, B. Y.; Wang, H.; Cai, S. Y.; Li, P.; Cai, W. W.; Ding, L. Y.; Yang, J.; Zheng, M.; Ren, J.; Zhang, Y. L.; Gao, J.; Xing, D.; Ren, N. Q.; Waymouth, R. M.; Zhou, J.; Tao, H. C.; Picard, C. J.; Benbow, M. E.; Criddle, C. S. Ubiquity of polystyrene digestion and biodegradation within yellow mealworms, larvae of *Tenebrio molitor* Linnaeus (Coleoptera: Tenebrionidae). *Chemosphere* **2018**, *212*, 262–271.
- (7) Yang, S.-S.; Brandon, A. M.; Andrew Flanagan, J. C.; Yang, J.; Ning, D.; Cai, S. Y.; Fan, H. Q.; Wang, Z. Y.; Ren, J.; Benbow, E.; Ren, N. Q.; Waymouth, R. M.; Zhou, J.; Criddle, C. S.; Wu, W.-M. Biodegradation of polystyrene wastes in yellow mealworms (larvae of *Tenebrio molitor* Linnaeus): factors affecting biodegradation rates and the ability of polystyrene-fed larvae to complete their life cycle. *Chemosphere* **2018**, *191*, 979–989.
- (8) Haider, T. P.; Völker, C.; Kramm, J.; Landfester, K.; Wurm, F. R. Plastics of the future? The impact of biodegradable polymers on the environment and on society. *Angew. Chem., Int. Ed.* **2019**, *58*, 50–62.
- (9) Wu, W. M.; Yang, J.; Criddle, C. S. Microplastics pollution and reduction strategies. *Front. Environ. Sci. Eng.* **2017**, *11*, No. 6.
- (10) Wang, L.; Wu, W.-M.; Bolan, N. S.; Tsang, D. C. W.; Li, Y.; Qin, M.; Hou, D. Environmental fate, toxicity and risk management strategies of nanoplastics in the environment: current status and future perspectives. *J. Hazard. Mater.* **2021**, *401*, No. 123415.
- (11) Wei, R.; Tiso, T.; Bertling, J.; O'Connor, K.; Blank, L. M.; Bornscheuer, U. T. Possibilities and limitations of biotechnological plastic degradation and recycling. *Nat. Catal.* **2020**, *3*, 867–871.
- (12) Inderthal, H.; Tai, S. L.; Harrison, S. T. L. Non-hydrolyzable plastics—an interdisciplinary look at plastic bio-oxidation. *Trends Biotechnol.* **2021**, *39*, 12–23.
- (13) Mills, J.; Klausmeier, R. F. The biodeterioration of synthetic polymers and plasticizers. *Crit. Rev. Environ. Sci. Technol.* **1974**, *4*, 341–351.
- (14) Shah, A. A.; Hasan, F.; Hameed, A.; Ahmed, S. Biological degradation of plastics: a comprehensive review. *Biotechnol. Adv.* **2008**, *26*, 246–65.
- (15) Min, K.; Cuiffi, J. D.; Mathers, R. T. Ranking environmental degradation trends of plastic marine debris based on physical properties and molecular structure. *Nat. Commun.* **2020**, *11*, No. 727.
- (16) Restrepo-Flórez, J.-M.; Bassi, A.; Thompson, M. R. Microbial degradation and deterioration of polyethylene—a review. *Int. Biodeterior. Biodegrad.* **2014**, *88*, 83–90.
- (17) Wu, W.-M.; Criddle, C. S. Characterization of biodegradation of plastics in insect larvae. *Methods Enzymol.* **2021**, *648*, 95–120.
- (18) Yang, Y.; Yang, J.; Wu, W.-M.; Zhao, J.; Song, Y.; Gao, L.; Yang, R.; Jiang, L. Biodegradation and mineralization of polystyrene by plastic-eating mealworms: part 1. chemical and physical characterization and isotopic tests. *Environ. Sci. Technol.* **2015**, *49*, 12080–12086.
- (19) Yang, S.-S.; Wu, W.-M. Biodegradation of Plastics in *Tenebrio* Genus (Mealworms). In *Microplastics in Terrestrial Environments*; Springer: Cham, 2020; Vol. 95, pp 385–422.
- (20) Yang, S.-S.; Ding, M.-Q.; Zhang, Z.-R.; Ding, J.; Bai, S.-W.; Cao, G.-L.; Zhao, L.; Pang, J.-W.; Xing, D.-F.; Ren, N.-Q.; Wu, W.-M. Confirmation of biodegradation of low-density polyethylene in dark-versus yellow- mealworms (larvae of *Tenebrio obscurus* versus *Tenebrio molitor*) via gut microbe-independent depolymerization. *Sci. Total Environ.* **2021**, *789*, No. 147915.
- (21) Yang, S.-S.; Ding, M. Q.; He, L.; Zhang, C. H.; Li, Q. X.; Xing, D. F.; Cao, G. L.; Zhao, L.; Ding, J.; Ren, N. Q.; Wu, W.-M. Biodegradation of polypropylene by yellow mealworms (*Tenebrio molitor*) and superworms (*Zophobas atratus*) via gut-microbe-dependent depolymerization. *Sci. Total Environ.* **2021**, *756*, No. 144087.
- (22) Yang, L.; Gao, J.; Liu, Y.; Zhuang, G.; Peng, X.; Wu, W.-M.; Zhuang, X. Biodegradation of expanded polystyrene and low-density polyethylene foams in larvae of *Tenebrio molitor* Linnaeus (Coleoptera: Tenebrionidae): broad versus limited extent depolymerization and microbe-dependence versus independence. *Chemosphere* **2021**, *262*, No. 127818.
- (23) Wang, Z.; Xin, X.; Shi, X.; Zhang, Y. A polystyrene-degrading *Acinetobacter* bacterium isolated from the larvae of *Tribolium castaneum*. *Sci. Total Environ.* **2020**, *726*, No. 138564.
- (24) Brandon, A. M.; Garcia, A. M.; Khlystov, N. A.; Wu, W. M.; Criddle, C. S. Enhanced bioavailability and microbial biodegradation of polystyrene in an enrichment derived from the gut microbiome of *Tenebrio molitor* (mealworm larvae). *Environ. Sci. Technol.* **2021**, *55*, 2027–2036.
- (25) Brandon, A. M.; Gao, S. H.; Tian, R.; Ning, D.; Yang, S. S.; Zhou, J.; Wu, W. M.; Criddle, C. S. Biodegradation of polyethylene and plastic mixtures in mealworms (larvae of *Tenebrio molitor*) and effects on the gut microbiome. *Environ. Sci. Technol.* **2018**, *52*, 6526–6533.
- (26) Brandon, A. M.; El Abbadi, S. H.; Ibekwe, U. A.; Cho, Y. M.; Wu, W. M.; Criddle, C. S. Fate of hexabromocyclododecane (HBCD), a common flame retardant, in polystyrene-degrading mealworms: elevated HBCD levels in egested polymer but no bioaccumulation. *Environ. Sci. Technol.* **2020**, *54*, 364–371.
- (27) Yang, S.-S.; Ding, M. Q.; Ren, X. R.; Zhang, Z. R.; Li, M. X.; Zhang, L. L.; Pang, J. W.; Chen, C. X.; Zhao, L.; Xing, D. F.; Ren, N. Q.; Ding, J.; Wu, W.-M. Impacts of physical-chemical property of polyethylene (PE) on depolymerization and biodegradation in insects yellow mealworms (*Tenebrio molitor*) and dark mealworms (*Tenebrio obscurus*) with high purity microplastics. *Sci. Total Environ.* **2022**, *828*, No. 154458.
- (28) Woo, S.; Song, I.; Cha, H. J. Fast and facile biodegradation of polystyrene by the gut microbial flora of *Plesiophthalmus davidi* larvae. *Appl. Environ. Microbiol.* **2020**, *86*, No. e01361-20.
- (29) Peng, B.-Y.; Su, Y.; Chen, Z.; Chen, J.; Zhou, X.; Benbow, M. E.; Criddle, C.; Wu, W.-M.; Zhang, Y. Biodegradation of polystyrene by dark (*Tenebrio obscurus*) and yellow (*Tenebrio molitor*) mealworms (Coleoptera: Tenebrionidae). *Environ. Sci. Technol.* **2019**, *53*, 5256–5265.
- (30) Peng, B.-Y.; Li, Y.; Fan, R.; Chen, Z.; Chen, J.; Brandon, A. M.; Criddle, C. S.; Zhang, Y.; Wu, W.-M. Biodegradation of low-density polyethylene and polystyrene in superworms, larvae of *Zophobas atratus* (Coleoptera: Tenebrionidae): broad and limited extent depolymerization. *Environ. Pollut.* **2020**, *266*, No. 115206.
- (31) Peng, B.-Y.; Chen, Z.; Chen, J.; Zhou, X.; Wu, W.-M.; Zhang, Y. Biodegradation of polylactic acid by yellow mealworms (larvae of *Tenebrio molitor*) via resource recovery: a sustainable approach for waste management. *J. Hazard. Mater.* **2021**, *416*, No. 125803.
- (32) Peng, B.-Y.; Chen, Z.; Chen, J.; Yu, H.; Zhou, X.; Criddle, C. S.; Wu, W.-M.; Zhang, Y. Biodegradation of polyvinyl chloride (PVC) in *Tenebrio molitor* (Coleoptera: Tenebrionidae) larvae. *Environ. Int.* **2020**, *145*, No. 106106.
- (33) LeMoine, C. M. R.; Grove, H. C.; Smith, C. M.; Cassone, B. J. A very hungry caterpillar: polyethylene metabolism and lipid

- homeostasis in larvae of the greater wax moth (*Galleria mellonella*). *Environ. Sci. Technol.* **2020**, *54*, 14706–14715.
- (34) Lou, Y.; Ekaterina, P.; Yang, S.-S.; Lu, B.; Liu, B.; Ren, N.; Corvini, P. F.-X.; Xing, D. Biodegradation of polyethylene and polystyrene by greater wax moth larvae (*Galleria mellonella* L.) and the effect of co-diet supplementation on the core gut microbiome. *Environ. Sci. Technol.* **2020**, *54*, 2821–2831.
- (35) Peng, B.-Y.; Sun, Y.; Wu, Z.; Chen, J.; Shen, Z.; Zhou, X.; Wu, W.-M.; Zhang, Y. Biodegradation of polystyrene and low-density polyethylene by *Zophobas atratus* larvae: fragmentation into microplastics, gut microbiota shift, and microbial functional enzymes. *J. Cleaner Prod.* **2022**, *367*, No. 132987.
- (36) Liu, J.; Liu, J.; Xu, B.; Xu, A.; Cao, S.; Wei, R.; Zhou, J.; Jiang, M.; Dong, W. Biodegradation of polyether-polyurethane foam in yellow mealworms (*Tenebrio molitor*) and effects on the gut microbiome. *Chemosphere* **2022**, *304*, No. 135263.
- (37) Tsochatzis, E. D.; Berggreen, I. E.; Vidal, N. P.; Roman, L.; Gika, H.; Corredig, M. Cellular lipids and protein alteration during biodegradation of expanded polystyrene by mealworm larvae under different feeding conditions. *Chemosphere* **2022**, *300*, No. 134420.
- (38) Thévenot, A.; Rivera, J. L.; Wilfart, A.; Maillard, F.; Hassouna, M.; Senga-Kiesse, T.; Le Féon, S.; Aubin, J. Mealworm meal for animal feed: Environmental assessment and sensitivity analysis to guide future prospects. *J. Cleaner Prod.* **2018**, *170*, 1260–1267.
- (39) van Broekhoven, S.; Oonincx, D. G.; van Huis, A.; van Loon, J. J. Growth performance and feed conversion efficiency of three edible mealworm species (Coleoptera: Tenebrionidae) on diets composed of organic by-products. *J. Insect Physiol.* **2015**, *73*, 1–10.
- (40) Yang, Y.; Yang, J.; Wu, W.-M.; Zhao, J.; Song, Y.; Gao, L.; Yang, R.; Jiang, L. Biodegradation and mineralization of polystyrene by plastic-eating mealworms: part 2. role of gut microorganisms. *Environ. Sci. Technol.* **2015**, *49*, 12087–12093.
- (41) Qin, L.; Duan, Z.; Cheng, H.; Wang, Y.; Zhang, H.; Zhu, Z.; Wang, L. Size-dependent impact of polystyrene microplastics on the toxicity of cadmium through altering neutrophil expression and metabolic regulation in zebrafish larvae. *Environ. Pollut.* **2021**, *291*, No. 118169.
- (42) Duan, Z.; Duan, X.; Zhao, S.; Wang, X.; Wang, J.; Liu, Y.; Peng, Y.; Gong, Z.; Wang, L. Barrier function of zebrafish embryonic chorions against microplastics and nanoplastics and its impact on embryo development. *J. Hazard. Mater.* **2020**, *395*, No. 122621.
- (43) Sanchez-Hernandez, J. C. A toxicological perspective of plastic biodegradation by insect larvae. *Comp. Biochem. Physiol., Part C: Toxicol. Pharmacol.* **2021**, *248*, No. 109117.
- (44) Wang, Y.; Zhang, Y. Investigation of gut-associated bacteria in *Tenebrio molitor* (Coleoptera: Tenebrionidae) larvae using culture-dependent and DGGE methods. *Ann. Entomol. Soc. Am.* **2015**, *108*, 941–949.
- (45) Li, P.; Oyang, X.; Xie, X.; Li, Z.; Yang, H.; Xi, J.; Guo, Y.; Tian, X.; Liu, B.; Li, J.; Xiao, Z. Phytotoxicity induced by perfluoroctanoic acid and perfluorooctane sulfonate via metabolomics. *J. Hazard. Mater.* **2020**, *389*, No. 121852.
- (46) Li, R.; Li, T.; Wan, Y.; Zhang, X.; Liu, X.; Li, R.; Pu, H.; Gao, T.; Wang, X.; Zhou, Q. Efficient decolorization of azo dye wastewater with polyaniline/graphene modified anode in microbial electrochemical systems. *J. Hazard. Mater.* **2022**, *421*, No. 126740.
- (47) Yang, X.; Zhou, J.; Huo, T.; Lv, Y.; Pan, J.; Chen, L.; Tang, X.; Zhao, Y.; Liu, H.; Gao, Q.; Liu, S. Metabolic insights into the enhanced nitrogen removal of anammox by montmorillonite at reduced temperature. *Chem. Eng. J.* **2021**, *410*, No. 128290.
- (48) Yang, L.; Su, Q.; Si, B.; Zhang, Y.; Zhang, Y.; Yang, H.; Zhou, X. Enhancing bioenergy production with carbon capture of microalgae by ultraviolet spectrum conversion via graphene oxide quantum dots. *Chem. Eng. J.* **2022**, *429*, No. 132230.
- (49) Wei, J.; Li, X.; Xiang, L.; Song, Y.; Liu, Y.; Jiang, Y.; Cai, Z. Metabolomics and lipidomics study unveils the impact of polybrominated diphenyl ether-47 on breast cancer mice. *J. Hazard. Mater.* **2020**, *390*, No. 121451.
- (50) Zhang, Y.; Liu, M.; Peng, B.; Jia, S.; Koh, D.; Wang, Y.; Cheng, H. S.; Tan, N. S.; Warth, B.; Chen, D.; Fang, M. Impact of Mixture Effects between emerging organic contaminants on cytotoxicity: a systems biological understanding of synergism between tris(1,3-dichloro-2-propyl)phosphate and triphenyl phosphate. *Environ. Sci. Technol.* **2020**, *54*, 10722–10734.
- (51) Chalamacharla, R. B.; Harsha, K.; Sheik, K. B.; Viswanatha, C. K. Wheat bran-composition and nutritional quality: a review. *Adv. Biotechnol. Microbiol.* **2018**, *9*, No. 555754.
- (52) Gaytán, I.; Sánchez-Reyes, A.; Burelo, M.; Vargas-Suárez, M.; Liachko, I.; Press, M.; Sullivan, S.; Cruz-Gómez, J.; Loza-Tavera, H. Degradation of recalcitrant polyurethane and xenobiotic additives by a selected landfill microbial community and its biodegradative potential revealed by proximity ligation-based metagenomic analysis. *Front. Microbiol.* **2020**, *10*, No. 2986.
- (53) Song, Y.; Qiu, R.; Hu, J.; Li, X.; Zhang, X.; Chen, Y.; Wu, W.-M.; He, D. F. Biodegradation and disintegration of expanded polystyrene by land snails *Achatina fulica*. *Sci. Total Environ.* **2020**, *746*, No. 141289.

□ Recommended by ACS

Water-Soluble Synthetic Polymers: Their Environmental Emission Relevant Usage, Transport and Transformation, Persistence, and Toxicity

Dongbo Wang, Xuran Liu, et al.

APRIL 13, 2023

ENVIRONMENTAL SCIENCE & TECHNOLOGY

READ ↗

Screening the Degradation of Polymer Microparticles on a Chip

Seyed Mohammad Davachi, Alireza Abbaspourrad, et al.

DECEMBER 23, 2022

ACS OMEGA

READ ↗

Biodegradation and Carbon Resource Recovery of Poly(butylene adipate-co-terephthalate) (PBAT) by Mealworms: Removal Efficiency, Depolymerization Patter...

Bo-Yu Peng, Yalei Zhang, et al.

JANUARY 26, 2023

ACS SUSTAINABLE CHEMISTRY & ENGINEERING

READ ↗

Environmental Biodegradation of Water-Soluble Polymers: Key Considerations and Ways Forward

Michael Zumstein, Michael Sander, et al.

AUGUST 05, 2022

ACCOUNTS OF CHEMICAL RESEARCH

READ ↗

Get More Suggestions >